Quinone-Enhanced Reduction of Nitric Oxide by Xanthine/Xanthine Oxidase

ARTICLE *in* CHEMICAL RESEARCH IN TOXICOLOGY · APRIL 2009

Impact Factor: 3.53 · DOI: 10.1021/tx800392j · Source: PubMed

Published in final edited form as:
Chem Res Toxicol. 2009 May ; 22(5): 818–823. doi:10.1021/tx800392j.

Quinone-Enhanced Reduction of Nitric Oxide by Xanthine/Xanthine Oxidase

Pedro Sanchez-Cruz and **Antonio E. Alegría***
Department of Chemistry, University of Puerto Rico at Humacao, Humacao, Puerto Rico 00791

Abstract

The quinones 1,4-naphthoquinone, methyl-1,4-naphthoquinone, tetramethyl-1,4-benzoquinone, 2,3-dimethoxy-5-methyl-1,4-benzoquinone, 2,6-dimethylbenzoquinone, 2,6-dimethoxybenzoquinone, and 9,10-phenanthraquinone enhance the rate of nitric oxide reduction by xanthine/xanthine oxidase in nitrogen-saturated phosphate buffer (pH 7.4). Maximum initial rates of NO reduction (V_{max}) and the amount of nitrous oxide produced after 5 min of reaction increase with quinone one- and two-electron redox potentials measured in acetonitrile. One of the most active quinones of those studied is 9,10-phenanthraquinone with a V_{max} value 10 times larger than that corresponding to the absence of quinone, under the conditions of this work. Because NO production is enhanced under hypoxia and under certain pathological conditions, the observations obtained in this work are very relevant to such conditions.

Introduction

Quinones form the second largest class of antitumor agents approved for clinical use in the United States, and several antitumor quinones are in different stages of clinical and preclinical development (1). A common feature in quinone-containing drugs is their ability to undergo reversible redox reactions to form semiquinone and oxygen radicals (2,3). One-electron reduction of a quinone (Q) gives the semiquinone radical ($Q^{\cdot-}$ or QH), while two-electron reduction gives the hydroquinone (QH_2) (3). The semiquinone can also be formed by a comproportionation reaction between a quinone and a hydroquinone; see reaction 1 (the opposite of reaction 1 is the semiquinone disproportionation reaction).

$$QH_2 + Q \rightarrow 2Q^{\cdot-} + 2H^+ \quad (1)$$

Quinones can be enzymatically reduced by flavoenzymes. Some of these can catalyze a one-electron reduction of quinones such as NADPH-cytochrome P450 reductase, NADH-cytochrome b_5 reductase, or NADH/NADH dehydrogenase (4,5). Xanthine oxidase (XO)[1] catalyzes the reduction of quinones by one and two electrons (6,7). The catalytic enhancement of ascorbate oxidation by quinones has been previously observed, including its dependence on the quinone one-electron redox potential (E^1_7) (8).

Nitric oxide is a free radical formed in a variety of cell types by NO synthase and has many important physiological roles such as acting as a vasorelaxant (9) and a neurotransmitter (10) and performing other physiological and pathophysiological phenomena (11). The one-electron reduced derivative of NO, the nitroxyl anion, $^3NO^-$ (or its conjugate acid, ^1HNO), is also a

*To whom correspondence should be addressed. antonio.alegria1@upr.edu.

vasorelaxant and inotropic and lusitropic agent (12). Because of the large pK_a value of ^{1}HNO, ca. 11.6, the conjugated acid, ^{1}HNO, is postulated the only significant reduced NO species under physiological conditions (13,14). Although nitroxyl increases postischemia/reperfusion in vivo injury (15), it can induce early preconditioning-like effects that protect heart tissue against ischemia-reperfusion injury (16), depending on the timing of administration (15). Because of the high reactivity of ^{1}HNO with thiols, ^{1}HNO is known to inactivate important enzymes such as the glycolytic enzyme glyceraldehyde 3-phosphate dehydrogenase (GAPDH) (17) and other cysteine-containing enzymes (12). Although ^{1}HNO toxicity has been found, this has been detected mostly at relatively high ^{1}HNO concentrations (18).

In a previous work, we have found that quinones increase the ascorbate anaerobic reduction extent of NO to form ^{1}HNO at physiological pH and that this enhancement is larger as the quinone one-electron redox potential increases (19). Other reports postulating NO reduction to ^{1}HNO have been published, including direct reduction of NO by species of the electron transport system in mitochondria (20,21), cytochrome *c* (22), ubiquinol (23), manganese superoxide dismutase (24), and XO (25). In addition, a possible role of quinone/hydroquinone redox system in the presence of NO and phenolic compounds in inducing DNA single strand breaks was postulated (26). XO was found to convert nitric oxide released from spermine-NONOate to nitroxyl in the presence of its substrate hypoxanthine (HX) under anaerobic conditions (25). In addition, evidence was found in that work that supported XO inhibition by ^{1}HNO. However, outersphere electron transfer mechanisms to NO are not likely to be physiologically possible due to the highly negative redox potential of NO (13).

---

^{1}Abbreviations:

NQ 1,4-naphthoquinone

MNQ methyl-1,4-naphthoquinone

DQ tetramethyl-1,4-benzoquinone

UBQ-0 2,3-dimethoxy-5-methyl-1,4-benzoquinone

DMBQ 2,6-dimethylbenzoquinone

DMOBQ 2,6-dimethoxybenzoquinone

PHQ 9,10-phenanthraquinone

HX hypoxanthine

XO xanthine oxidase

DPI diphenyliodonium chloride

DPV differential pulse voltammetry

ROS reactive oxygen species

EPR electron paramagnetic resonance

Quinones are known to enhance reactive oxygen species (ROS) production in the XO-catalyzed oxidation of xanthine (X) or HX (27-29). Here, we have extended our work regarding the quinone-enhanced reduction of NO by determining the kinetic parameters for the X/XO reduction of NO in the presence and absence of quinones. This work was done under anaerobic conditions as an approximation of hypoxic regions in tissues under abnormal conditions or of events of reduced oxygen supply, such as ischemia. Because NO production is enhanced under hypoxic conditions in several tissues (30,31), it is under those conditions where NO reduction to ^{1}HNO should be more relevant. The use of XO is relevant to the bioreductive activation of quinones. XO is found in endothelial cells (32), likely to be active in tumor cells (33), and is also found in nuclei (34).

Materials and Methods

Chemicals

X, XO (EC 1.1.3.22), and quinones were purchased from Sigma Chemical Company (St. Louis, MO). Diphenyliodonium chloride (DPI) was purchased from Aldrich (St. Louis, MO). Quinones (Figure 1) were purified by double sublimation before use. These quinones were selected since they have a wide range of redox potentials, are commercialy available, and are found to be active in the enhanced reduction of oxygen by ascorbate (8). Stock solutions of quinones were freshly prepared in DMSO or water depending on the quinone water solubility, although the amount of DMSO in samples was always kept below 0.2%. High-purity N_2 was used to deareate solutions. Nitric oxide was prepared by addition of a N_2-saturated KNO_2 solution to an excess of a N_2-saturated KI solution in H_2SO_4. The NO gas produced was passed through N_2-saturated 5 M NaOH to remove any higher oxides of nitrogen and dissolved into ice-cooled, N_2-saturated water. Nitrous oxide was obtained from Puritan Medical Products. Only distilled, deionized, and Chelex- treated water was used in this work. Chelex treatment of water was monitored using the ascorbate test, as described by Buettner (35). Care was always taken to minimize exposure of quinone-containing solutions to light.

Nitric Oxide Reduction Kinetics

These were monitored using a NO-specific electrochemical probe (ISO-NOP) inserted in a thermostatted NO chamber (World Precision Instruments, Sarasota, FL) at 37 °C. The chamber was purged with high-purity nitrogen followed by injection of 1.00 mL of a nitrogen-saturated solution containing 20 μM NO, 10 mU XO/mL, and 50 μM X from 0 to 20 μM quinone in 50 mM phosphate buffer (pH 7.4). This was followed by immediate exclussion of all gas bubbles out of the sample, through the chamber capillary. Nitric oxide was then added in the absence of a gas phase in the sample. The sample was continuously stirred using a spinning bar. Data acquisition was started after NO addition. X was the last reagent added. Basal voltage was calibrated to zero every day. Voltage output corresponding to a 20 μM NO solution was checked every day, and the electrode membrane was replaced in case there was not agreement with previous outputs within 10%. The electrode was calibrated daily with known concentrations of $NaNO_2$ by reacting this salt with KI in sulfuric acid medium. NO consumption data were collected in a computer, and the initial rates of NO consumption (R_{NO}) were measured.

Nitrous Oxide Determination

A volume of 1.00 mL of a N_2-saturated solution containing 100 μM quinone,100 mU XO/mL, 50 mM phosphate buffer (pH 7.4), 650 μM NO, and 450 μM X was stirred in the thermostated NO chamber at 37 °C for 5 min. This was followed by addition of 100 μM allopurinol to inhibit XO. A sample of the gaseous phase was then withdrawn from the reaction vessel and injected in the gas chromatograph. Nitrous oxide was detected using an Agilent 6890 gas chromatograph equipped with a Porapak Q column (6′ × 1/8”) and a thermal conductivity detector operating

at 40 °C with a flow rate of 7 mL/min. The N_2O peak was identified using a standard of N_2O from a lecture bottle.

To determine the mol ratio of N_2O produced to that of NO consumed, a nitrogen-saturated reaction mixture containing 40 μM quinone, 100 mU XO/mL, and 450 μM X in 50 mM phosphate buffer at pH 7.4 (X was added last) was reacted in the thermostated chamber at 37 °C until all of the NO was consumed, as detected from the electrode reading. At this point, 50 μL of the headspace was injected in the GC for analysis. Quantification of N_2O production was performed at 37 °C by determining the total amount of N_2O in the gas and aqueous phases using the reported Henry's constant for N_2O at this temperature (36) to obtain the amount at the liquid phase.

Determination of Half-Wave Reduction Potentials ($E_{1/2}$)

These were determined in nitrogen-purged acetonitrile solutions containing 1 mM quinone and 0.1 M tetra-*n*-butylammonium perchlorate (TBAP) using differential pulse voltammetry (DPV). A BAS CV 50W voltammetric analyzer using a glassy carbon working electrode was used in these determinations. An Ag/AgCl(sat) electrode was used as the reference electrode (E' = +0.22 V vs NHE) and a platinum wire as the counter electrode. Differential pulse voltammograms were obtained in the potential range of -2.00 to 0.00 V, using a 50 mV pulse amplitude and 20 mV/s scan rate. The reduction potential values were obtained from the DPV peak potential maxima. These were almost similar to the half-wave redox potentials, $E_{1/2}$, in normal polarographic measurements (37).

Results and Discussion

Nitric Oxide Reduction Kinetics

Changes in NO levels as a function of time in the reaction mixtures containing NO and X/XO in N_2-saturated phosphate buffer in the absence and presence of various quinones were monitored using the NO-specific electrode. An example is shown in Figure 2 corresponding to 2,3-dimethoxy-5-methyl-1,4-benzoquinone (UBQ-0). Initial rates were measured from the initial slope of the [NO] traces. In the absence of quinone, a relatively small change in the NO levels as a function of time was noted in the reaction mixture containing NO and X/XO. However, when quinones are included in this reaction, a relatively fast decrease of NO was noted. Nonlinear regressions of the Michaelis-Menten equation, that is, of plots of R_{NO} (after subtracting the NO consumption rate in the absence of quinone) vs the quinone concentration, produced the Michaelis-Menten constants, K_m, and maximum rates, V_{max} (Figure 3 and Table 1). Values of V_{max} correlate with quinone $E_{1/2}$ potentials determined in this work (Figure 4). 9,10-Phenanthraquinone (PHQ) was found to be one of the most active quinones, showing a V_{max} value 10 times larger than that in the absence of quinone, under the conditions of this work. Second-order polynomials were found to better fit the plots in Figure 4 (see the Figure 4 caption) than other functions (linear, exponential, and third and fourth degree polynomials). However, the physical cause of this observation is at present unknown. The addition of DPI, an inhibitor of the XO flavin site (38), inhibits from 94 to 97% NO reduction in samples containing quinone, X/XO, and NO (Figure 2). This observation, coupled to the observed enhancement in NO consumption and N_2O production, indicates that electrons are being transferred from this site to the quinone. The latter then shuttles electrons to NO.

The formation of N_2O is unambiguous evidence for ^{1}HNO production or NO reduction and has been used as the sole evidence of ^{1}HNO in several works (39-44). Headspace sampling of the nitrogen-saturated reaction mixture containing NO, X, and XO in the presence or absence of quinone demonstrated the formation of N_2O as determined by GC. The amount of N_2O detected after 5 min of initiating the reaction was also found to increase with the quinone redox

potential (Figure 5). As found for plots in Figure 4, second-order polynomials were found to better fit plots in Figure 5 (see the Figure 5 caption) than other functions (linear, exponential, and third and fourth degree polynomials). Again, the physical cause of this observation is at present unknown. All of the quinones used in this work enhance the formation of N_2O as compared to $(3.0 \pm 0.5) \times 10^{-10}$ mol of N_2O produced in the absence of quinone.

Nitrous oxide is being produced due to either the reaction of ^{1}HNO with NO (reaction 2) or the ^{1}HNO dimerization followed by dehydration (reaction 3) (45,46).

$$^1\text{HNO} + 2\text{NO} \rightarrow \text{N}_2\text{O} + \text{HNO}_2 \quad (2)$$

$$^1\text{HNO} + {}^1\text{HNO} \rightarrow \text{N}_2\text{O} + \text{H}_2\text{O} \quad (3)$$

The measured mol ratios of N_2O produced to that of NO consumed, corresponding to samples of all of the quinones studied, were found to be in the range between 0.19 and 0.26 (Table 1). Dimerization of ^{1}HNO to produce N_2O is a relatively slow process, and it is thus likely that N_2O is formed mostly from reaction 2. Indeed, the expected stoichiometry for this process (mol N_2O appearing/mol NO disappearing) is predicted to be 0.33, that is, from NO + $1e^-$ → ^{1}HNO followed by reaction 2. The expected value is somewhat larger than those obtained in this work. Thus, it seems that either some of the ^{1}HNO is also reacting with some of the sample components before forming N_2O or a small fraction of the consumed NO is not due to reduction. As indicated above, it has been reported that the ^{1}HNO produced partially inhibits XO (25), although other constituents of our samples could also be reacting with a fraction of the ^{1}HNO produced. The latter will be a matter of further study in our research group. Addition of 100 μM GSH to the samples inhibits N_2O production from 94 to 100% but not NO consumption, in accordance with the high reactivity of thiols with ^{1}HNO (47). Furthermore, addition of 100 μM DPI to the samples inhibits N_2O production from 95 to 100% and from 94 to 97% NO consumption, indicating that quinone reduction occurs at the flavin site of the enzyme. This observation united to the quinone-enhanced NO reduction proves that quinones are shuttling electrons from the XO $FADH^+$ to NO.

The hydroquinone derivatives of these quinones, that is, the two-electron reduced products, could also be involved in this electron transfer process. For example, the hydroquinone of UBQ-0 has been reported to reduce NO with a rate constant of 4.9×10^5 M^{-1} s^{-1} (23). In addition, X/XO can act as both a one- or two-electron donor (48). Correlations obtained in the present work between the V_{max} or the amount of N_2O produced and the first- and second-electron redox potentials suggest that both the semiquinone and the hydroquinone could be responsible for NO reduction in the present work (Figures 4 and 5).

Although several works, as indicated above, suggest direct reduction of NO by biologically relevant molecules, it has been argued that NO cannot be reduced directly by common biological reducing agents since the NO redox potential is too negative. From the pK_a value of 11.6 for ^{1}HNO ($^1\text{HNO} \rightarrow {}^3\text{NO}^- + \text{H}^+$), a potential of about -0.5 V (1 M vs NHE) has been estimated for the reduction of NO to $^3NO^-$ and subsequent protonation to ^{1}HNO at pH 7.2 (13). Thus, direct reduction of NO by X [two-electron oxidation potential = +0.360 V (1 M vs NHE) to form uric acid (49)] should not be probable. However, it is recognized that a given redox reaction with a negative redox potential will occur if some of its products is used in other reactions (50). Formation of N_2O and its release into the gaseous phase could be such reaction. However, a possibility for NO reduction, without these large energy barriers, could involve an inner sphere reduction of NO whereby the semiquinone or other species involved in the

reduction process, such as X, XO, and/or quinone, forms a complex with NO followed by electron transfer from the semiquinone to NO. The possible interaction of NO with those species is a matter of a near future study. Furthermore, at relatively high concentrations of NO, a dimer is formed, which is more prone for reduction [+ 0.33 V vs NHE (13)]. Even though quinones also have negative one-electron redox potentials relative to NHE (51), these catalyze the NO reduction reaction as they do in ascorbate- or X-to-oxygen electron transfer reactions, as stated above.

The value of 11.6 for the pK_a of $^3NO^-$ is for the formation of ^1HNO. This protonation is a spin-forbidden process, and it is highly likely that, even with such a high pK_a, the $^3NO^-$ exhibits a long lifetime, which has been estimated in the order of milliseconds (14). Thus, $^3NO^-$could react with other species, in particular, with two NO molecules to generate N_2O and HNO_2 (reaction 2). This would mean that the protonation of $^3NO^-$ should not be occurring at conditions where NO is in excess.

In summary, the quinones under study here enhance the X/XO reduction of NO. Both the V_{max} values and the amount of nitroxyl produced after 5 min of reaction increase with the quinone one- and two-electron reduction potentials. In view of the fact that NO production is enhanced under hypoxia and under certain pathological conditions (52-54), the observations obtained in this work should even be more relevant under such conditions.

Acknowledgment

We express appreciation for Grants SO6-GM008216 and P20RR-16470 for financial support of this work.

References

(1). Boyle RG, Travers S. Hypoxia: targeting the tumour. Anticancer Agents Med. Chem 2006;6:281–286. [PubMed: 16842231]

(2). O'Brien PJ. Molecular mechanisms of quinone cytotoxicity. Chem.-Biol. Interact 1991;80:1–41. [PubMed: 1913977]

(3). Tudor G, Gutierrez P, Aguilera-Gutierrez A, Sausville EA. Cytotoxicity and apoptosis of benzoquinones: Redox cycling, cytochrome c release, and BAD protein expression. Biochem. Pharmacol 2003;65:1061–1075. [PubMed: 12663042]

(4). Tani N, Yabuki M, Komuro S, Kanamaru H. Characterization of the enzymes involved in the in vitro metabolism of amrubicin hydrochloride. Free Radical Res 2001;35:145–158. [PubMed: 11697195]

(5). Iyanagi T, Yamazaki I. One-electron reduction in biochemical systems. V. Difference in the mechanism of quinone reduction by NADH dehydrogenase and the NAD(P)H dehydrogenase (DT-diaphorase). Biochim. Biophys. Acta 1970;216:282–294. [PubMed: 4396182]

(6). Alegria AE, Santiago G. Adriamycin and daunomycin semiquinone membrane/buffer partition constants using the spin-broadening technique. Arch. Biochem. Biophys 1997;346:91–95. [PubMed: 9328288]

(7). Schreiber J, Mottley C, Sinha BK, Kalyanaraman B, Mason RP. One-electron reduction of daunomycin, daunomycinone and 7-deoxydaunomycinone by xanthine/xanthine oxidase system: Detection of semiquinone free radicals by electron spin resonance. J. Am. Chem. Soc 1987;109:348–351.

(8). Roginsky VA, Barsukova TK, Stegmann HB. Kinetics of redox interaction between substituted quinones and ascorbate under aerobic conditions. Chem.-Biol. Interact 1999;121:177–197. [PubMed: 10418963]

(9). Dessy C, Moniotte S, Ghisdal P, Havaux X, Noirhomme P, Balligand JL. Endothelial beta3-adrenoceptors mediate vasorelaxation of human coronary microarteries through nitric oxide and endothelium-dependent hyperpolarization. Circulation 2004;110:948–954. [PubMed: 15302798]

(10). Gomes MZ, Raisman-Vozari R, Del Bel EA. A nitric oxide synthase inhibitor decreases 6-hydroxydopamine effects on tyrosine hydroxylase and neuronal nitric oxide synthase in the rat nigrostriatal pathway. Brain Res 2008;1203:160–169. [PubMed: 18313645]

(11). Lancaster JR Jr. Simulation of the diffusion and reaction of endogenously produced nitric oxide. Proc. Natl. Acad. Sci. U.S.A 1994;91:8137–8141. [PubMed: 8058769]

(12). Paolocci N, Jackson MI, Lopez BE, Miranda K, Tocchetti CG, Wink DA, Hobbs AJ, Fukuto JM. The pharmacology of nitroxyl (HNO) and its therapeutic potential: Not just the Janus face of NO. Pharmacol. Ther 2007;113:442–458. [PubMed: 17222913]

(13). Bartberger MD, Liu W, Ford E, Miranda KM, Switzer C, Fukuto JM, Farmer PJ, Wink DA, Houk KN. The reduction potential of nitric oxide (NO) and its importance to NO biochemistry. Proc. Natl. Acad. Sci. U.S.A 2002;99:10958–10963. [PubMed: 12177417]

(14). Shafirovich V, Lymar SV. Nitroxyl and its anion in aqueous solutions: spin states, protic equilibria, and reactivities toward oxygen and nitric oxide. Proc. Natl. Acad. Sci. U.S.A 2002;99:7340–7345. [PubMed: 12032284]

(15). Ma XL, Gao F, Liu GL, Lopez BL, Christopher TA, Fukuto JM, Wink DA, Feelisch M. Opposite effects of nitric oxide and nitroxyl on postischemic myocardial injury. Proc. Natl. Acad. Sci. U.S.A 1999;96:14617–14622. [PubMed: 10588754]

(16). Pagliaro P, Mancardi D, Rastaldo R, Penna C, Gattullo D, Miranda KM, Feelisch M, Wink DA, Kass DA, Paolocci N. Nitroxyl affords thiol-sensitive myocardial protective effects akin to early preconditioning. Free Radical Biol. Med 2003;34:33–43. [PubMed: 12498977]

(17). Norris AJ, Sartippour MR, Lu M, Park T, Rao JY, Jackson MI, Fukuto JM, Brooks MN. Nitroxyl inhibits breast tumor growth and angiogenesis. Int. J. Cancer 2008;122:1905–1910. [PubMed: 18076071]

(18). Fukuto JM, Jackson MI, Kaludercic N, Paolocci N. Examining nitroxyl in biological systems. Methods Enzymol 2008;440:411–431. [PubMed: 18423233]

(19). Alegria AE, Sanchez S, Quintana I. Quinone-enhanced ascorbate reduction of nitric oxide: Role of quinone redox potential. Free Radical Res 2004;38:1107–1112. [PubMed: 15512799]

(20). Clarkson RB, Norby SW, Smirnov A, Boyer S, Vahidi N, Nims RW, Wink DA. Direct measurement of the accumulation and mitochondrial conversion of nitric oxide within Chinese hamster ovary cells using an intracellular electron paramagnetic resonance technique. Biochim. Biophys. Acta 1995;1243:496–502. [PubMed: 7727525]

(21). Zhao XJ, Sampath V, Caughey WS. Cytochrome c oxidase catalysis of the reduction of nitric oxide to nitrous oxide. Biochem. Biophys. Res. Commun 1995;212:1054–1060. [PubMed: 7626092]

(22). Sharpe MA, Cooper CE. Reactions of nitric oxide with mitochondrial cytochrome c: A novel mechanism for the formation of nitroxyl anion and peroxynitrite. Biochem. J 1998;332(Part 1):9–19. [PubMed: 9576846]

(23). Poderoso JJ, Carreras MC, Schopfer F, Lisdero CL, Riobo NA, Giulivi C, Boveris AD, Boveris A, Cadenas E. The reaction of nitric oxide with ubiquinol: Kinetic properties and biological significance. Free Radical Biol. Med 1999;26:925–935. [PubMed: 10232836]

(24). Niketic V, Stojanovic S, Nikolic A, Spasic M, Michelson AM. Exposure of Mn and FeSODs, but not Cu/ZnSOD, to NO leads to nitrosonium and nitroxyl ions generation which cause enzyme modification and inactivation: An in vitro study. Free Radical Biol. Med 1999;27:992–996. [PubMed: 10569631]

(25). Saleem M, Ohshima H. Xanthine oxidase converts nitric oxide to nitroxyl that inactivates the enzyme. Biochem. Biophys. Res. Commun 2004;315:455–462. [PubMed: 14766230]

(26). Ohshima H, Gilibert I, Bianchini F. Induction of DNA strand breakage and base oxidation by nitroxyl anion through hydroxyl radical production. Free Radical Biol. Med 1999;26:1305–1313. [PubMed: 10381204]

(27). Osman AM, van Noort PC. Evidence for redox cycling of lawsone (2-hydroxy-1,4-naphthoquinone) in the presence of the hypoxanthine/xanthine oxidase system. J. Appl. Toxicol 2003;23:209–212. [PubMed: 12884402]

(28). Alegria AE, Cordones E, Santiago G, Marcano Y, Sanchez S, Gordaliza M, Martin-Martin ML. Reductive activation of terpenylnaphthoquinones. Toxicology 2002;175:167–175. [PubMed: 12049845]

(29). Monteiro HP, Vile GF, Winterbourn CC. Release of iron from ferritin by semiquinone, anthracycline, bipyridyl, and nitroaromatic radicals. Free Radical Biol. Med 1989;6:587–591. [PubMed: 2753390]

(30). Serrano J, Encinas JM, Fernandez AP, Rodrigo J, Martinez A. Effects of acute hypobaric hypoxia on the nitric oxide system of the rat cerebral cortex: Protective role of nitric oxide inhibitors. Neuroscience 2006;142:799–808. [PubMed: 16952423]

(31). Yamamoto Y, Henrich M, Snipes RL, Kummer W. Altered production of nitric oxide and reactive oxygen species in rat nodose ganglion neurons during acute hypoxia. Brain Res 2003;961:1–9. [PubMed: 12535770]

(32). White CR, Darley-Usmar V, Berrington WR, McAdams M, Gore JZ, Thompson JA, Parks DA, Tarpey MM, Freeman BA. Circulating plasma xanthine oxidase contributes to vascular dysfunction in hypercholesterolemic rabbits. Proc. Natl. Acad. Sci. U.S.A 1996;93:8745–8749. [PubMed: 8710942]

(33). Chekulayeva L, Shevchuk I, Chekulayev V, Oginskaya E. Influence of heating on the activity of xanthine oxidase in tumor cells subjected to the phototoxic action of hematoporphyrin derivative. Neoplasma 2007;54:229–234. [PubMed: 17447855]

(34). Pritsos CA. Cellular distribution, metabolism and regulation of the xanthine oxidoreductase enzyme system. Chem.-Biol. Interact 2000;129:195–208. [PubMed: 11154741]

(35). Buettner GR. In the absence of catalytic metals ascorbate does not autoxidize at pH 7: Ascorbate as a test for catalytic metals. J. Biochem. Biophys. Methods 1988;16:27–40. [PubMed: 3135299]

(36). Bensetiti Z, Iliuta I, Larachi F, Grandjean BPA. Solubility of nitrous oxide in amine solutions. Ind. Eng. Chem. Res 1999;38:328–332.

(37). Sawyer, DT.; Roberts, JL. Experimental Electrochemistry for Chemists. Wiley and Sons; New York: 1974.

(38). Li H, Samouilov A, Liu X, Zweier JL. Characterization of the effects of oxygen on xanthine oxidase-mediated nitric oxide formation. J. Biol. Chem 2004;279:16939–16946. [PubMed: 14766900]

(39). Singh RJ, Hogg N, Joseph J, Kalyanaraman B. Photosensitized decomposition of S-nitrosothiols and 2-methyl-2-nitrosopropane. Possible use for site-directed nitric oxide production. FEBS Lett 1995;360:47–51. [PubMed: 7875299]

(40). Yoo J, Fukuto JM. Oxidation of N-hydroxyguanidine by nitric oxide and the possible generation of vasoactive species. Biochem. Pharmacol 1995;50:1995–2000. [PubMed: 8849325]

(41). Nagasawa HT, Kawle SP, Elberling JA, DeMaster EG, Fukuto JM. Prodrugs of nitroxyl as potential aldehyde dehydrogenase inhibitors vis-a-vis vascular smooth muscle relaxants. J. Med. Chem 1995;38:1865–1871. [PubMed: 7783118]

(42). Turk T, Hollocher TC. Oxidation of dithiothreitol during turnover of nitric oxide reductase: Evidence for generation of nitroxyl with the enzyme from Paracoccus denitrificans. Biochem. Biophys. Res. Commun 1992;183:983–988. [PubMed: 1567412]

(43). Fukuto JM, Wallace GC, Hszieh R, Chaudhuri G. Chemical oxidation of N-hydroxyguanidine compounds. Release of nitric oxide, nitroxyl and possible relationship to the mechanism of biological nitric oxide generation. Biochem. Pharmacol 1992;43:607–613. [PubMed: 1540216]

(44). Garber EA, Hollocher TC. Positional isotopic equivalence of nitrogen in N2O produced by the denitrifying bacterium *Pseudomonas stutzeri*. Indirect evidence for a nitroxyl pathway. J. Biol. Chem 1982;257:4705–4708. [PubMed: 7068659]

(45). Fukuto JM, Hszieh R, Gulati P, Chiang KT, Nagasawa HT. N,O-Diacylated-N-hydroxyarylsulfonamides: Nitroxyl precursors with potent smooth muscle relaxant properties. Biochem. Biophys. Res. Commun 1992;187:1367–1373. [PubMed: 1417812]

(46). Wink, DA.; Feelisch, M. Formation and detection of nitroxyl and nitrous oxide. In: Feelisch, M.; Stamler, JS., editors. Methods in Nitric Oxide Research. John Wiley & Sons Ltd.; London: 1996. p. 403-412.

(47). Miranda KM, Paolocci N, Katori T, Thomas DD, Ford E, Bartberger MD, Espey MG, Kass DA, Feelisch M, Fukuto JM, Wink DA. A biochemical rationale for the discrete behavior of nitroxyl and nitric oxide in the cardiovascular system. Proc. Natl. Acad. Sci. U.S.A 2003;100:9196–9201. [PubMed: 12865500]

(48). Fridovich I. Quantitative aspects of the production of superoxide anion radical by milk xanthine oxidase. J. Biol. Chem 1970;245:4053–4057. [PubMed: 5496991]

(49). Burton K. Free energy data of biological interest. Ergeb. Physiol. Biol. Chem. Exp. Pharmakol 1957;49:275–285.

(50). Buettner GR. The pecking order of free radicals and antioxidants: lipid peroxidation, alpha-tocopherol, and ascorbate. Arch. Biochem. Biophys 1993;300:535–543. [PubMed: 8434935]

(51). Wardman P. Reduction potentials of one-electron couples involving free radicals in aqueous solution. J. Phys. Chem. Ref. Data 1989;18:1637–1755.

(52). Wahl SM, McCartney-Francis N, Chan J, Dionne R, Ta L, Orenstein JM. Nitric oxide in experimental joint inflammation. Benefit or detriment? Cells Tissues Organs 2003;174:26–33. [PubMed: 12784039]

(53). Datta N, Mukherjee S, Das L, Das PK. Targeting of immunostimulatory DNA cures experimental visceral leishmaniasis through nitric oxide up-regulation and T cell activation. Eur. J. Immunol 2003;33:1508–1518. [PubMed: 12778468]

(54). Grisham MB, Pavlick KP, Laroux FS, Hoffman J, Bharwani S, Wolf RE. Nitric oxide and chronic gut inflammation: controversies in inflammatory bowel disease. J. Invest. Med 2002;50:272–283.

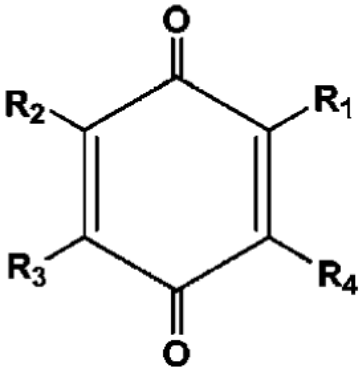

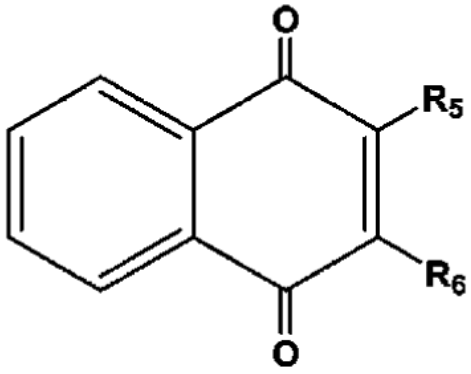

DMBQ; $R_1 = R_2 = CH_3$, $R_3 = R_4 = H$
UBQ-0; $R_1 = CH_3$, $R_2 = R_3 = OCH_3$, $R_4 = H$
DMOBQ; $R_1 = R_2 = OCH_3$, $R_3 = R_4 = H$
DQ; $R_1 = R_2 = R_3 = R_4 = CH_3$

NQ; $R_5 = R_6 = H$
MNQ; $R_5 = CH_3$, $R_6 = H$

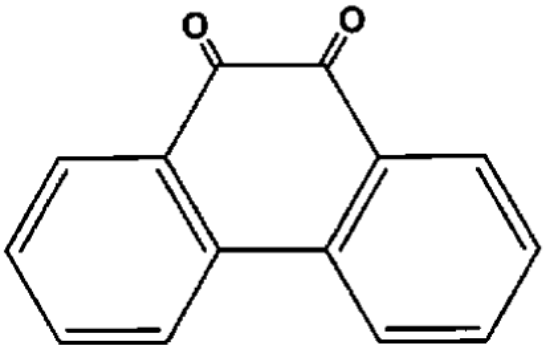

PHQ

Figure 1.
Quinones used in this study.

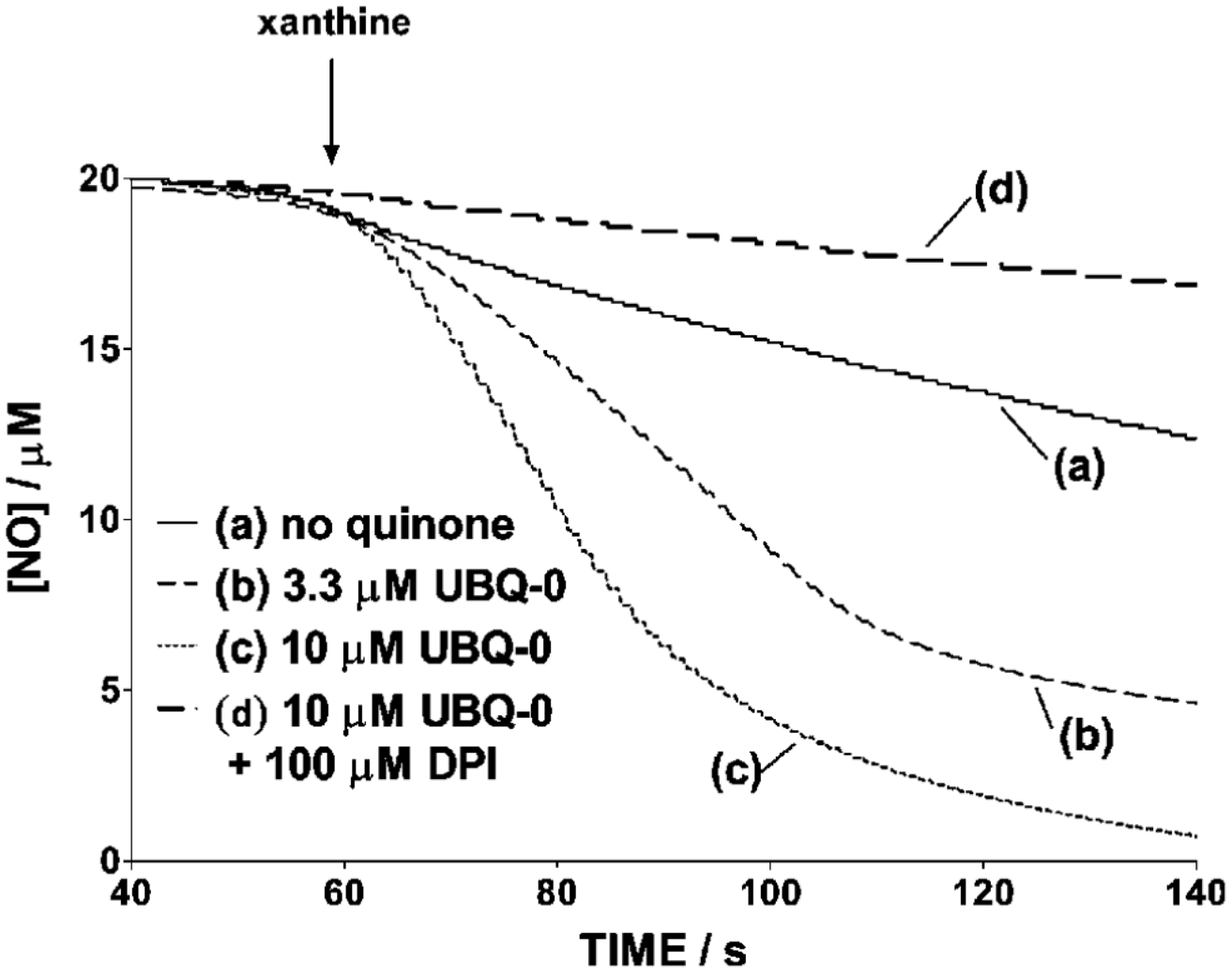

Figure 2.

Nitric oxide concentration traces occurring in N_2-saturated samples containing 20 μM NO, 10 mU XO/mL, and 50 μM X in the presence or absence of UBQ-0 and in the absence and presence of 100 μM DPI, in 50 mM phosphate buffer (pH 7.4) at 37 °C. The arrow indicates the instant where X was injected to the sample. Runs in this figure were made the same day, and representative curves are shown.

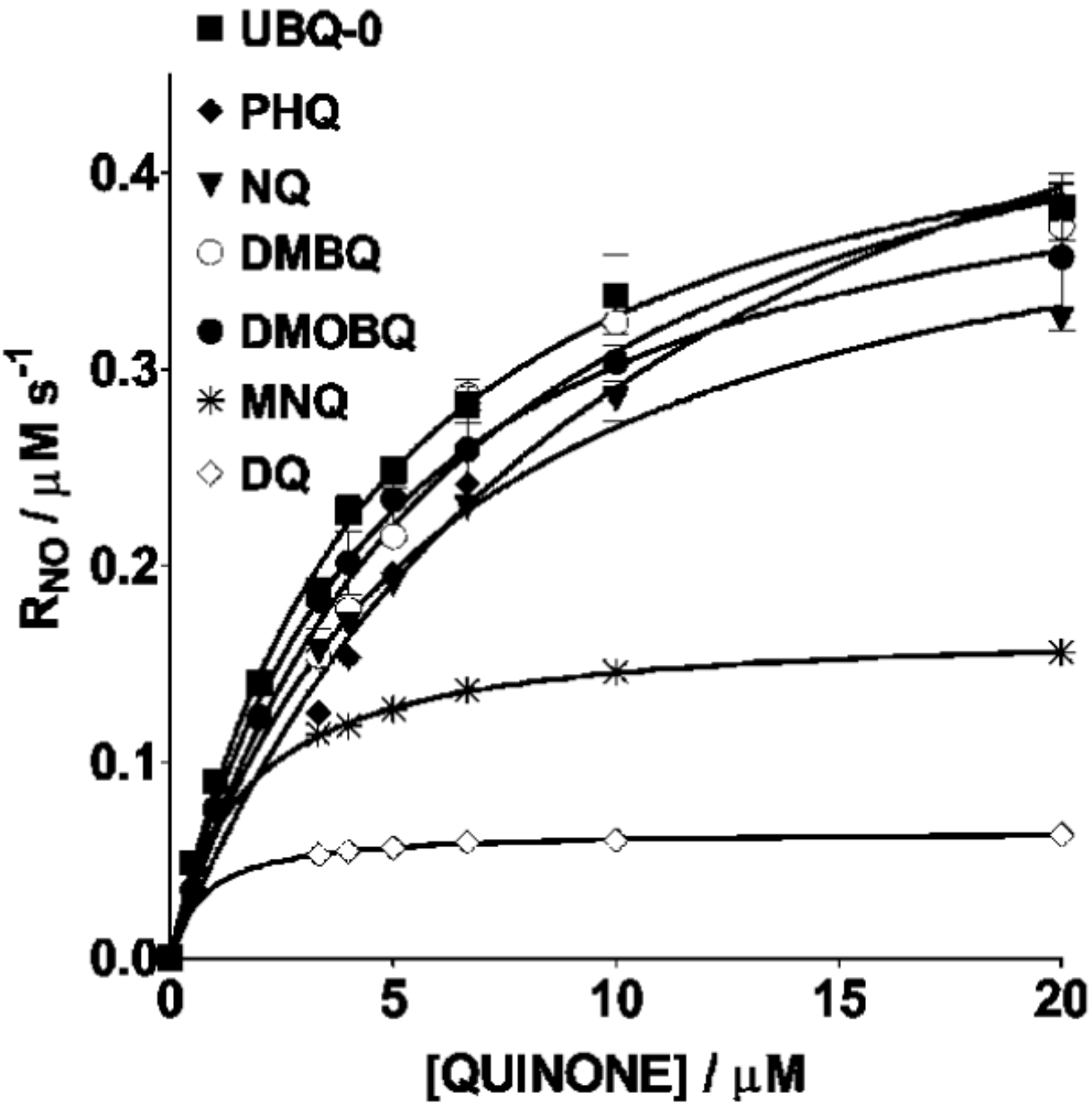

Figure 3.

Michael-Menten plots used to determine V_{max} and K_m for the X/XO reduction of NO in the presence of quinones. Samples were N_2-saturated solutions containing 20 μM NO, 10 mU XO/mL, 50 μM X, and 50 mM phosphate buffer (pH 7.4) and in the presence of 3.33-20 μM quinone. The temperature is 37 °C. Initial rates of NO consumption used were those obtained after subtracting the basal initial rate, that is, in the absence of quinone, $(6.2 \pm 0.3) \times 10^{-8}$ M/s' from the measured initial rate. Error bars are standard errors of the mean value of at least three determinations.

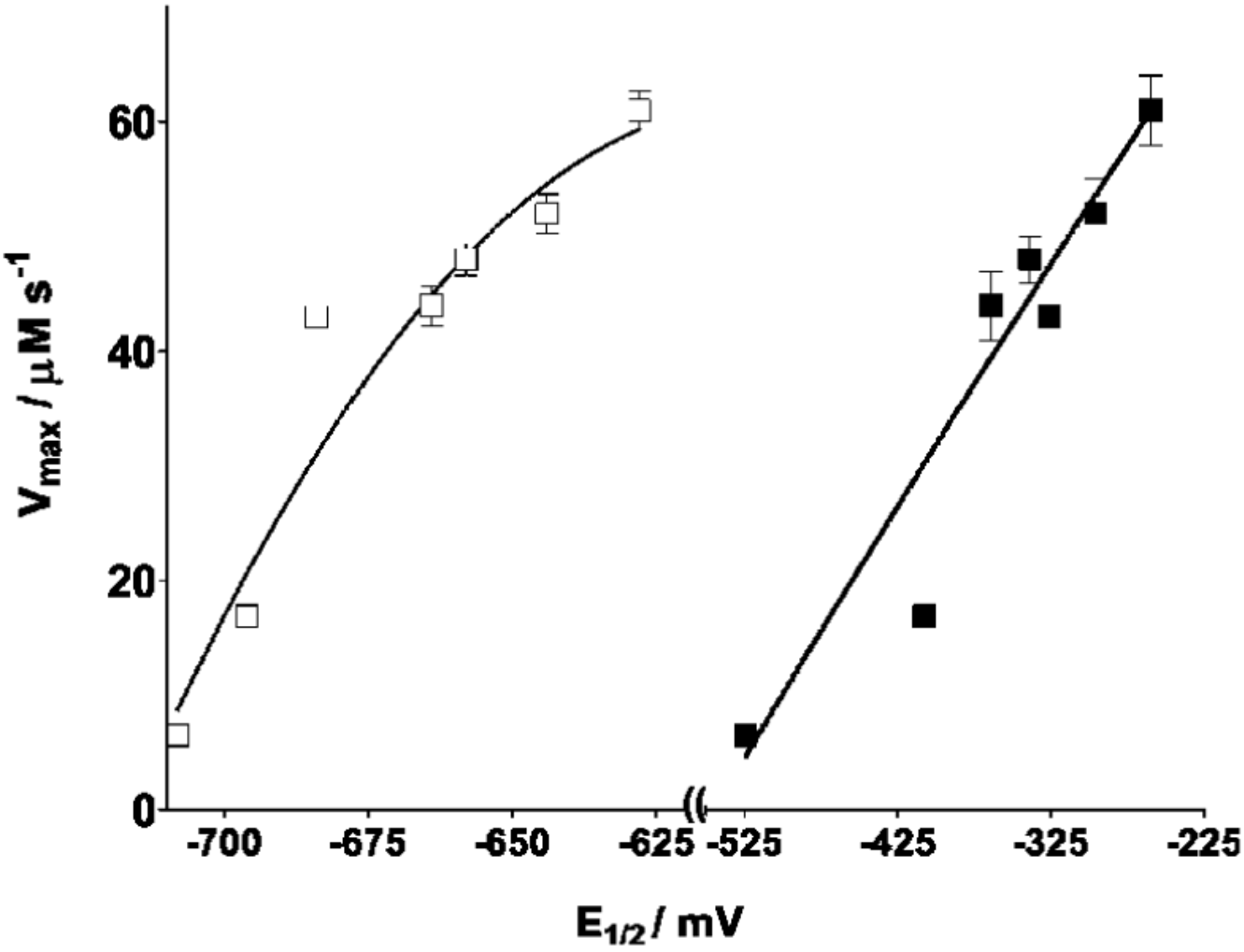

Figure 4.

Dependence of V_{max} values on the first (closed circles) and second (open circles) quinone redox potentials. V_{max} values were obtained from nonlinear regressions of plots in Figure 3. Sample compositions are stated in the Figure 3 caption. Error bars are standard errors of the mean values of at least three determinations. Nonlinear regressions of second-order polynomials were used for the curves shown here. Goodness-of-fit values (R^2) of 0.99 and 0.99 were obtained for plots against first and second electron redox potentials, respectively.

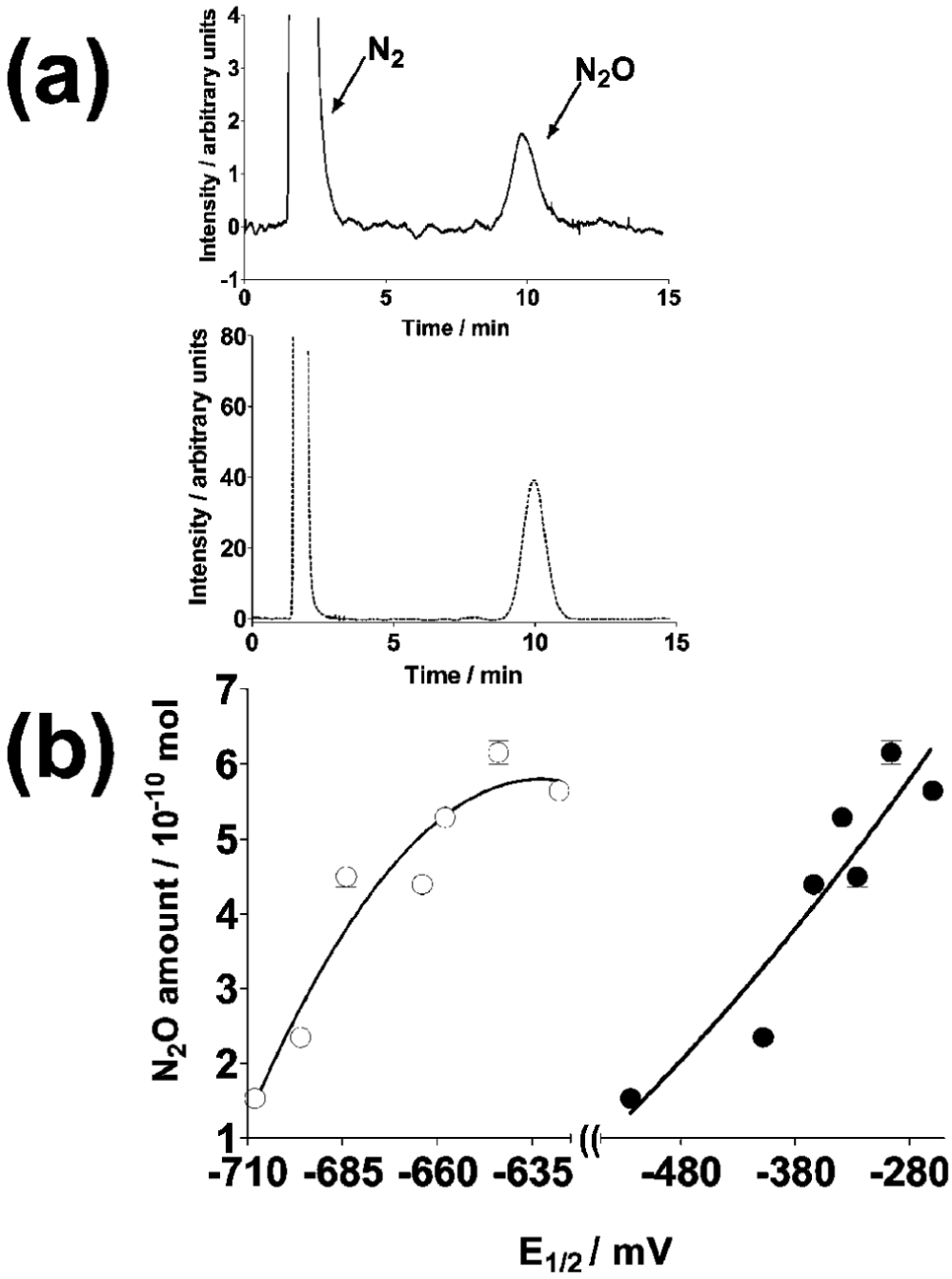

Figure 5.

(a) GC chromatograms of a diluted N_2O standard (dotted line) and that in the head space of a sample (continuous line) with the composition stated below and UBQ-0 as the quinone. (b) Dependence of the N_2O amount in the head space of samples, after subtraction of that in the absence of quinone, on the first (closed circles) and second (open circles) quinone redox potentials. Samples were nitrogen-saturated reaction mixtures containing 100 μM quinone,100 mU XO/mL, 50 mM phosphate buffer (pH 7.4), 650 μM NO, and 450 μM X after 5 min of reaction at 37 °C. The amount of N_2O obtained in the absence of quinone after 5 min of reaction is $(3.0 \pm 0.5) \times 10^{-10}$ moles. Error bars are standard errors of the mean values of at least three determinations. Nonlinear regressions of second-order polynomials were used for the curves

shown in panel b. Goodness-of-fit values (R^2) of 0.92 and 0.90 were obtained for plots against first and second electron redox potentials, respectively.

Table 1

Kinetic Parameters of the X/XO Reduction of NO in the Presence of Quinones and Ratio of N_2O Produced to That of NO Consumed[a]

quinone	$E_{1/2}$ (mV)[b]		K_m (μM)	V_{max}[c] (10^{-8} M s^{-1})	R^2[e]	N_2O/NO consumed[f]
PHQ	-260	-628	11 ± 1	61 ± 3[d]	0.99	0.26 ± 0.02
DMBQ	-296	-644	6.8 ± 0.9	52 ± 3	0.98	0.26 ± 0.03
NQ	-326	-684	5.9 ± 0.4	43 ± 1	0.99	0.23 ± 0.02
UBQ-0	-339	-658	4.6 ± 0.4	48 ± 2	0.97	0.26 ± 0.03
DMOBQ	-364	-664	4.7 ± 0.9	44 ± 3	0.89	0.24 ± 0.03
MNQ	-408	-696	1.6 ± 0.1	16.9 ± 0.2	0.998	0.20 ± 0.03
DQ	-524	-708	0.79 ± 0.04	6.54 ± 0.04	1.0	0.19 ± 0.02

[a] Nitrogen-saturated solutions containing 20 μM NO, 10 mU XO/mL, and 50 μM X from 0 to 20 μM quinone in 50 mM phosphate buffer (pH 7.4). Michaelis and Menten parameters, K_m and V_{max} were obtained from nonlinear correlations of Michaelis-Menten plots shown in Figure 3.

[b] Determined by DPV against an Ag/AgCl reference electrode at 25 °C in acetonitrile. Left and right columns correspond to the first and second electron redox potentials, respectively.

[c] Initial rates of NO consumption used to obtain K_m and V_{max} were those obtained after subtracting the basal initial rate, that is, in the absence of quinone, (6.2 ± 0.3) × 10^{-8} M/s' from the measured initial rate.

[d] Errors in V_{max} and K_m are those obtained from the corresponding nonlinear regressions.

[e] Goodness-of-fit values of Michaelis-Menten plot regressions.

[f] Mol ratios of N_2O produced to NO consumed. Errors are of the means of three determinations.